Heliyon 10 (2024) e28268

Contents lists available at ScienceDirect

Heliyon

journal homepage: www.cell.com/heliyon

Research article

An experimental evaluation of drying banana slices using a novel indirect solar dryer under variable conditions

Ashmore Mawire[a,*], Masodi Ramokali[a], Molebogeng Mothupi[a], Maarten Vanierschot[a,b]

[a] North-West University, Material Science, Innovation and Modelling (MaSIM) Research Focus Area, Department of Physics, Mmabatho, 2745, Mahikeng, South Africa
[b] KU Leuven, Department of Mechanical Engineering, Group T Leuven campus, Celestijnenlaan 300, B-3001, Heverlee, Belgium

ARTICLE INFO

Keywords:
Bananas
Different drying conditions
Solar dryer
Thermal performance characteristics

ABSTRACT

Novel thermal characteristics of drying banana slices in an indirect dryer are presented for four different experimental drying conditions in the forced convection mode. The novel characteristics include measuring the airflow velocity in the drying chamber, measuring the thermal profiles in different trays comprehensively and measuring the relative humidity under different conditions. Two tests are carried for 16 h in two consecutive days (8 h per day for each test). The first test is on acloudy day followed by a sunny day, while the second test is carried out on two consecutive sunny days. Tests 3 and 4 are 24 h tests with high (0.23 m/s) and low (0.11 m/s) average drying chamber airflow velocities under good solar radiation conditions. The maximum temperatures obtained in the collector and the drying chamber are around 80 and 48 °C, respectively, for the 16 h tests. Significantly lower collector and drying chamber temperatures are obtained due to cloudy conditions. Maximum collector temperatures are around 84 and 95 °C for the high and low average airflow chamber velocities for the 24 h tests. The corresponding maximum temperatures in the drying chamber are around 50 °C for the 24 tests. The final moisture ratios are 0.26 (cloudy and sunny days) and 0.20 (two sunny days), respectively, for the 16 h tests. These final moisture ratios are lower than those obtained for the 24 h tests which are 0.32 and 0.28, respectively. Increasing the drying chamber airflow velocity results in faster moisture removal during sunshine hours for the 24 h tests. For tests 1, 2, 3 and 4, the maximum average collector efficiencies during the sunshine period are around 60, 80, 40 and 10 %, respectively. The average drying efficiencies for the total solar drying period for tests 1,2,3 and 4 on day 1 are 6.9, 6.9, 5.5 and 5.7 % respectively. These values are comparable, suggesting that the average collector powers, airflow velocities and efficiencies have a very small effect on the average solar drying efficiency for the whole drying period. The quality of the bananas slices mainly in terms of the colour and shape is also compared with previous studies and commercially available products. A reasonably acceptable quality product is obtained.

1. Introduction

The adequate provision of a sustainable food supply chain is vital to human survival especially in the developing world which faces

* Corresponding author.
E-mail address: ashmore.mawire@nwu.ac.za (A. Mawire).

https://doi.org/10.1016/j.heliyon.2024.e28268
Received 13 September 2023; Received in revised form 6 March 2024; Accepted 14 March 2024
Available online 21 March 2024

Nomenclature

A_a	Cross-sectional area of blowing air [m^2]
A_c	Collector area [m^2]
c_a	Specific heat capacity of air [$Jkg^{-1}K^{-1}$]
H_w	Latent heat of vaporisation for water [JK^{-1}]
I	Global solar radiation [Wm^{-2})
I_{av}	Moving average global solar radiation [Wm^{-2}]
$\dot{m}_{av}$	Moving average mass flowrate of air [kgs^{-1}]
$\dot{m}_{wav}$	Hourly mass rate of water evaporated [kgs^{-1}]
M	Moisture content [kg]
M_0	Initial moisture content [kg]
M_{eq}	Equilibrium moisture content [kg]
MR	Moisture ratio [−]
T	Temperature [K]
T_{cin}	Collector inlet temperature [K]
T_{cout}	Collector outlet temperature [K]
$\dot{v}$	Airflow velocity [ms^{-1}]
$\dot{v}_{av}$	Moving average airflow velocity [ms^{-1}]
η_c	Solar collector thermal efficiency [−]
η_d	Solar drying efficiency [−]
ρ_a	Density of air [kgm^{-3}]

a lot of problems related for food security [1]. Developing countries are particularly prone to food shortages due to the ever-growing population, poor food preservation techniques and natural disasters such as floods and droughts [2,3]. The Food and Agriculture Organization (FAO) of the United Nations reported in 2011 that close to 1.3 billion tonnes of food produced for human consumption are lost annually [4]. Due to these high food losses, mainly because of improper food preservation techniques, people from low income developing countries are often suffering from malnutrition [5].

Drying of food is one of the energy intensive techniques that can preserve it for a long-time, reducing post harvesting losses experienced by subsistence farmers in the developing world. Food drying with using the open sun is the cheapest and most widely used drying method in the developing world which has lot of disadvantages such as non-controlled moisture removal resulting in over- and under-drying and contamination and spoilage of food products because of wind, dust, excessive solar radiation exposure and rain [6]. In addition to this, drying in the open sun has other problems which are; (1) the labour-intensive nature of the process requiring consistent monitoring in a large area for a long period of time, (2) food is prone to insect infestation, (3) food sometimes losses nutrients and colouring and (4) moisture re-absorption in the food during non-sunshine periods when food is on the ground. To cater for most of the drawbacks of open sun drying, controlled direct and indirect solar drying in recent years has been widely reviewed in detail, and different designs have been presented in recent comprehensive reviews on solar dryers [7–10]. Food that has been dried in solar dryers includes fruits and vegetables [11], sugarcane [12] and meat [13]. Of particular interest in the developing world in Asia and Africa are fruits which are widely available naturally or farmed by both subsistence and commercial farmers which include grapes [14], apples [15], bananas [16,33], mangoes [17] and pineapples [18].

Bananas are widely farmed in Sub-Saharan Africa and are a relatively cheap form of food with a lot of nutritional benefits [19]. However, the problem with bananas is that they easily rot even with refrigeration. Drying for later use can be an alternative sustainable food preservation method for Sub-Saharan African farmers to reduce post-harvesting losses hence increasing food security. Some recent work has been presented on the solar drying of bananas due to their wide availability, cheap farming methods and nutritional value [20–29]. Amer et al. [20] experimentally evaluated a hybrid solar dryer for bananas. 30 kg of bananas were dried in 8 h from an initial moisture ratio of 72 %–18 % on a wet basis (wb) whereas open sun drying only showed a final moisture of 62 % in the same period. Nabnean and Nimnuan [21] presented the experimental performance of a direct forced convection household solar dryer. The moisture content of the bananas in the dryer was reduced from an initial value of 72 % (wb) to a final value of 28 % (wb) within 4 days, compared to 40 % (wb) using open sun drying. Moreover, the drying time was reduced by 48 %. Hedge et al. [22] presented an innovative solar dryer for drying bananas. Bananas dried at a volumetric flowrate of 0.0338 m^3/s using a collector air velocity of 1 m/s produced best quality compared to drying with 0.5 and 2 m/s. The quality was evaluated in terms of colour, taste and shape for the same solar energy input and atmospheric conditions. A double-sided solar collector drying unit for banana slices was fabricated and evaluated by Pruengam et al. [23]. The drying chamber achieved a maximum temperature of around 62.7 °C which was around 13.6 °C higher than drying naturally with the sun. The high drying rate of the solar collector dryer reduced the banana moisture content faster by 1.3–1.5 times compared to open sun drying.

An experimental study coupled with a computational fluid dynamics (CFD) analysis of drying bananas was presented by Mutabilwa and Nwaigwe [24]. A double pass solar collector (DPSC) was used in the experimental study, and experimental results compared well to numerical simulations. The dryer showed improved efficiency compared to other similar designs due its uniquely designed arrangement of components. Good quality dried banana chips were obtained, and the quality performance indicators were the taste, colour and shape. Arun et al. [25] presented active drying of unripe bananas in a multi-tray mixed mode solar cabinet dryer with backup energy storage. Untreated unripe bananas having an average of 180 % (dry basis) moisture content were tested. Drying experiments performed with tray sequencing achieved a moisture content below 18 % on a dry basis. Wakjira et al. [26] performed an experiment for determining the slice thickness of bananas for a solar cabinet under Ethiopian conditions. Experimental results revealed that as the thickness increased, the moisture content also increased, whereas the number of sticky and brown slices decreased. Mouldy slices were about 38 % when the thickness was greater than 6 mm compared to none for thicknesses between 1 and 4 mm. For a thickness of 5 mm, the percentage number of mouldy slices was around 3 %. After four days of the drying process, the moisture content was less 20 % for all banana slices except for the larger slices (5 and 6 mm). The optimal thicknesses for the solar dryer were 3 and 4 mm. The solar drying performance of peaches and bananas in Tunisia was presented by Narsi [27]. The work investigated a solar chimney-dryer for developing appropriate mathematical models for both bananas and peaches. For drying bananas, results showed that the Midilli and Kucuk model was the most appropriate model since it had the highest coefficient of determination (R^2) for both high and low air flow rates. Lingayat et al. [28] designed and developed an indirect solar dryer for drying bananas. The qualitative analysis for drying of bananas showed that moisture content of the bananas was reduced from an initial value of 356 % on a dry basis (db) to a final moisture content of 16, 19, 21, 31, and 42 % (db) for the four trays of the dryer, and for open sun drying respectively. A numerical investigation of an indirect solar dryer for banana chips drying together with energy and exergy analyses was performed by Lingayat and Chandramohan [29]. The average collector and dryer efficiencies obtained during the experimental tests were 64.50 and 55.30 %, respectively. Banana samples were dried from 3.5566 to 0.2604 kg/kg on a dry basis.

From the reviewed literature, it is clear that drying bananas with solar dryers results in better performance compared to open sun drying, however, there is still more experimental and numerical work that must be done to improve the performance of these solar dryers. This paper extends the previous work done on solar dryers for drying bananas by examining novel aspects that have been rarely investigated. Firstly, the proposed dryer has DC fans attached at the top of the collector reducing the dust that enters from the blower or fan placed at the bottom of the collector. Secondly, the airflow velocity profiles are measured both at the collector inlet and inside the drying chamber to fully understand the drying kinetics instead of the normal practice of measuring the airflow velocity at the inlet and outlet ports of the collector. Besides, the pressure drop in the collector makes the airflow velocity in the chamber different from the airflow velocity at the inlet and outlet ports. Therefore, knowledge of the airflow velocity in the chamber is essential for proper modelling of the drying kinetics in it. Thirdly, a detailed knowledge of the temperature distribution inside the collector and drying trays is essential to understand the drying capabilities and potential for drying different foods. This has also been rarely investigated in current literature. To compete with electrical dryers, a detailed knowledge of temperature distribution is required to understand the drying kinetics. Most previous work only focused on a limited number of measuring locations. The moisture ratio in each tray is also determined to understand the drying kinetics in more detail. Detailed thermal profiles can assist in selecting appropriate products to be put in the dryer as well as assessing the heat distribution in different sections of the dryer. Fourthly, this study compares the performance under different drying conditions. These different drying conditions contain different weather conditions and different periods of drying which include consecutive 16 h (8 h per day for two days) of solar radiation and continuous 24 h operation. A good dryer should be able to operate under variable conditions, and this has been rarely reported in the previous work on solar dryers for drying bananas. The collector and drying efficiencies are also evaluated using moving average values to understand the variation of the efficiencies which are different for non-ideal solar drying conditions. With issues of climate change, good drying solar conditions will

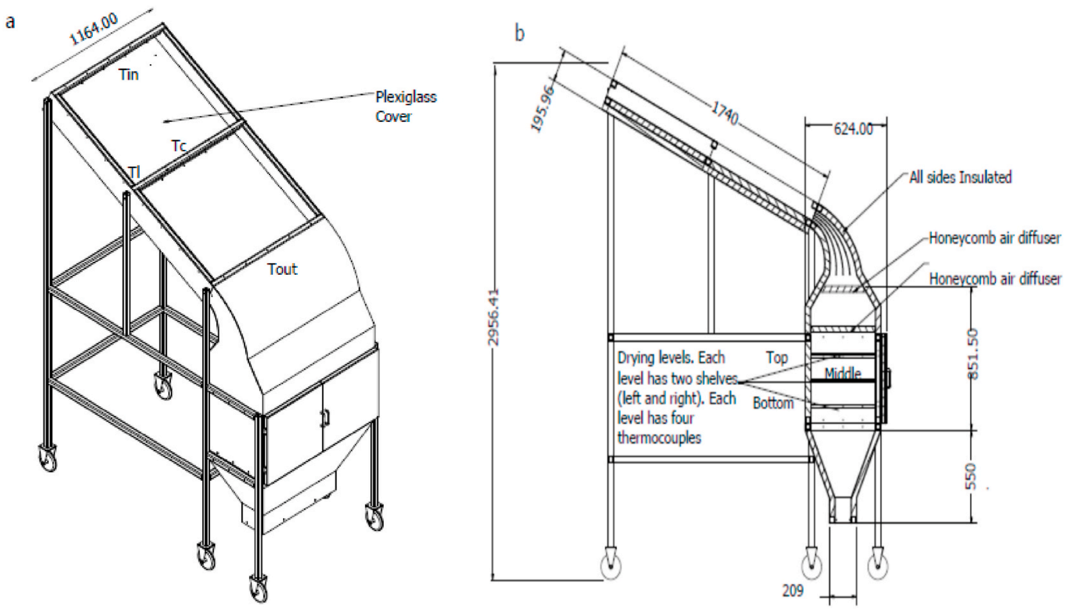

Fig. 1. (a) Isometric and (b) cross-sectional side views of the dryer with different components. The dimensions are in mm.

become scarce thus it is necessary to test a solar dryer under these non-ideal conditions. Finally, the quality mainly in terms of the colour and shape of the dried product is compared with previous rarely reported work and commercially available products. The papers presented in previous studies seem not to compare their dried products with commercially available products.

Solar drying is more appropriate and relevant to the developing world where there is limited access to electricity, people cannot afford electricity, and post harvesting losses of food products are high due to inappropriate food preservation methods such as open sun drying [6]. Besides this, the use of solar drying technologies assists in addressing at least five United Nations Sustainable Development Goals (SDGs) of No Poverty (SDG 1), Zero Hunger (SDG 2), Good Health and Well- Being (SDG 3), Clean and Affordable Energy (SDG 7) and Climate Change (SDG 13). It is essential for the developing world to promote the use of solar dryers instead of other types of food dryers such as electrical and biomass which are unsustainable in the long-run due to high electricity prices, unavailability of electricity in the developing world and greenhouse gas emissions.

In a bid to address these mentioned research gaps in the solar drying of bananas, an experimental study using a novel solar dryer is presented in this paper. Twelve thermocouples are inserted in the drying chamber at 2 different positions in each of the 6 trays to measure the temperature profiles inside the dryer. These profiles at the top, middle and bottom levels (with 2 trays per level) are measured during 16 h (8 h per day) of solar radiation and continuously during 24 h drying cycles. Results obtained will be useful in further optimising solar dryers for bananas. The quality of the dried banana slices is also compared with previous work and commercially available products to justify the adoption of the proposed solar drying solution.

2. Experimental setup and method

Fig. 1(a) and (b) are schematic diagrams showing the dimensions of the solar dryer in mm. The dryer is an upscaled version of the one reported by Tegenaw et al. [30] for field experimental testing. A stainless-steel absorber on a flat plate solar collector covered with Plexiglas captures incident solar radiation. The collector has a length of 1.740 m, and the highest point of the collector is 3 m from the ground. Six CPU fans at the inlet port are used to extract thermal energy generated due to solar radiation heating the absorber plate. Hot air extracted from the absorber is used to heat the drying chamber containing banana slices. The fans can be powered by a solar panel which charges a battery using a charge controller or with a DC power supply. A DC power supply was used to obtain a variable airflow velocity during experimental tests. A thermal switch in the charge controller prevented the solar panel from operating continuously for 24 h. It switched off the fans after 5 h, thus continuous 24 h operation using the battery was not possible. To obtain low (0.10 m/s) and high (0.20 m/s) average drying chamber air velocities, the DC power supply was set to DC currents of 0.2 and 0.4 A, respectively. Two flat K-thermocouples placed centrally on the absorber plate measured Tin and Tout, the inlet and outlet temperatures of the collector with an accuracy of ± 2 °C. To measure the central collector temperature (Tc), and the left-hand side (Tl) collector temperature on the central axis, two flat K-thermocouples were also used. Two honeycomb air diffusers before the drying chamber were used to improve heat transfer and uniformize the airflow.

The drying chamber consists of top, middle and bottom drying levels. A total of six trays/compartments are in the drying chamber, and each level has two trays (left and right). To measure the temperature distribution in each level, four K-thermocouples are placed on the trays (2 per tray). The accuracy of the thermocouples is ± 2 °C. Fig. 2 (a, b) shows a drying tray without and with bananas. A wire mesh with a pore size of 1 mm had to be added on top of the empty tray since the diameters of the banana slices were smaller than the pore size of the tray mesh (Fig. 2(b)) to ensure that the bananas do not fall during drying experiments due the larger pore size of the tray mesh. Each tray has a length and width of 51 cm and 47 cm, respectively. Two thermocouples are placed in each tray to measure the temperature distribution during drying. One thermocouple is at centre of the tray and another one at the central rear side edge of

Fig. 2. (a) An empty drying tray with central and rear side thermocouples and (b) banana slices loaded on a tray with a 1 mm wire mesh placed on top of the tray during experimentation.

the tray. Lemon juice was poured on the banana slices to limit the growth of microorganisms before the drying tests. Each tray had around 120–130 circular banana slices (disks) with thicknesses ranging from 4.5 to 5 mm. The slices had diameters which ranged from 25 to 30 mm, and 10 bananas are placed in each tray making a total mass of around 530 g in each tray. Bananas with a total mass of around 3.18 kg were placed in the six trays.

Fig. 3 shows a photograph of the solar dryer with the main components indicated. Two Testo 450i thermal anemometers measure the airflow velocity inside the drying chamber and at the inlet port of the collector. The anemometer has a measuring range of 0–30 m/s, and its resolution is 0.01 m/s. In the range of 0–2 m/s used in the experimental tests, the accuracy of the anemometer is± 0.01 m/s. A Kipp and Zonen CMP11 pyranometer measures the global solar radiation on the solar collector with a 95 % response time of less than 5 s. A Mastech 625 B anemometer measures the wind speed during drying experiments. It has a range of 0.8–30 m/s, resolution of 0.01 m/s and an accuracy that is± 2 % of the measured value. A Hession digital temperature and humidity meter with an accuracy of ±5 % measures the relative humidity at a resolution of 1 % of the measured value.

3. Experimental thermal analysis

Four drying experiments were carried out in October and November 2021 under different drying conditions. The first two tests were carried out with an average chamber air flow velocity of around 0.20 m/s under two consecutive days of 8 h of solar radiation (9:00–17:00 h) making a total 16 h of solar drying. For test 1 (29–30 October 2021), a cloudy day followed by sunny day were the weather conditions for solar drying. For test 2 (1–2 November 2021), two consecutive days of sunny 8 h periods were the conditions for the test. In the next two tests, continuous 24 h drying was carried out during sunshine and non-sunshine periods at night (from 9 a.m. day 1–9 a.m. day 2). The solar radiation was comparable for test 3 (3–4 November 2021) and test 4 (9–10 November 2021), however, test 3 was carried out with an average drying chamber air flow velocity of around 0.23 m/s in the drying chamber, and test 4 with an average air flow velocity of around 0.11 m/s in the chamber. An Agilent 34970 A datalogger connected to a computer recorded data from the thermocouples and the pyranometer during experimental drying tests. Manual measurements were taken hourly for the other remaining parameters. The total mass of the bananas was measured every hour by opening the dryer so that the moisture ratio could be estimated. The moisture ratio was estimated [31] as:

$$MR = \frac{M - M_{eq}}{M_0 - M_{eq}} \approx \frac{M}{M_0}, \tag{1}$$

where M is the moisture content, M_{eq} is the equilibrium moisture content and M_0 is the initial moisture content. M_{eq} is much less than M and M_0 therefore it can be neglected as indicated in Eq. (1).

The average solar collector thermal efficiency is calculated by the ratio of the average thermal collector output power to the average solar input power which can be expressed in Eq. (2) as [32,34]:

$$\eta_c = \frac{\dot{m}_{av} c_a (T_{cout} - T_{cin})}{I_{av} A_c} = \frac{\rho_a \dot{v}_{av} A_a c_a (T_{cout} - T_{cin})}{I_{av} A_c}, \tag{2}$$

where $\dot{m}_{av}$ is the moving average mass flowrate of air, c_a the specific heat capacity of air, T_{cout} is the collector outlet temperature, T_{cin} is collector inlet temperature, I_{av} is the moving average global solar radiation to cater for fluctuations during cloudy periods, A_c is the collector area, ρ_a is the density of air, $\dot{v}_{av}$ is the moving average airflow velocity through the collector to cater for periodic fluctuations in the airflow velocity, and A_a is the cross-sectional area of air blowing through the collector.

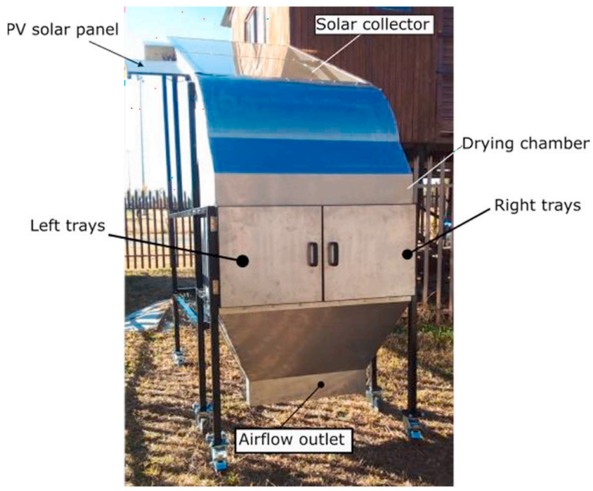

Fig. 3. A photograph of the solar dryer.

The solar drying efficiency is calculated from the ratio of the average hourly rate of water evaporated to average solar power input [32,34], and it is expressed in Eq. (3) as:

$$\eta_d = \frac{\dot{m}_{wav}\, H_w}{I_{av} A_c}, \tag{3}$$

where $\dot{m}_{wav}$ (kg/s) is the hourly mass rate of water evaporated and H_w (kJ/kg) is the latent heat of vapourisation for water, taken to be 2260 kJ/kg. The cumulative moving average global solar radiation can be calculated in Eq. (4) as [35]:

$$I_{av} = i = 1N\frac{I}{N}, \tag{4}$$

where N is the number of samples taken during an hourly measurement interval. In a similar manner, the moving average airflow velocity through the collector can be expressed in Eq. (5) as [35]:

$$\dot{v}_{av} = \sum_{i=1}^{N} \frac{\dot{v}}{N}. \tag{5}$$

4. Results and discussion

4.1. Solar drying tests on two consecutive days of solar radiation

The global solar radiation, windspeed and collector temperature profiles for the two 16 h tests during daytime hours are shown in Fig. 4. The tests were carried out during two consecutive days with 8 h intervals in each test day (9:00–17:00 h).

Fig. 4 (A1) shows a cloudy day test on the first day followed by a clear sky day on the second day. The average solar radiation on day 1 is around 706 W/m^2, whereas for day 2 it is around 943 W/m^2. In contrast to test 1, test 2 (Fig. 4 (A2)) shows two almost clear sky condition days. The average solar radiation for day 1 is around 975 W/m^2 which is comparable to that of day 2 (1005 W/m^2). The windspeeds for both tests fluctuate up and down for the duration of the experiments, and the maximum wind speed is close to 5 m/s for both tests. The average windspeeds during the 16 h periods are around 1.40 m/s for both tests.

Fig. 4(B1) shows the collector and ambient temperatures for test 1. As expected, the collector temperatures for day 1 fluctuate up and down due the fluctuating solar radiation conditions. The collector outlet temperature for day 1 reaches a maximum close to 80 °C

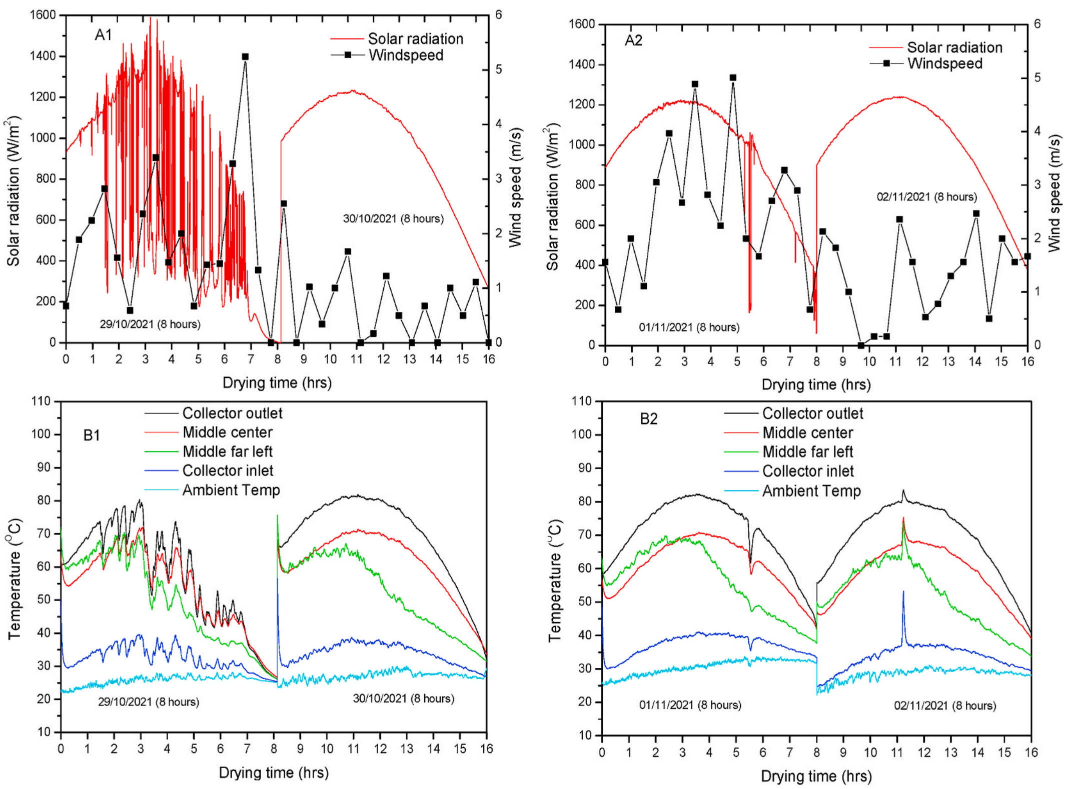

Fig. 4. (A) Global solar radiation and wind speed profiles and, (B) collector and ambient temperatures for 16 h in two consecutive days of drying with sun.

when the inlet temperature is around 40 °C. It also be observed that the middle centre temperature of the collector is greater than the middle far left temperature suggesting better heat transfer at the centre of the collector. In contrast to the plots of day 1, day 2 shows slightly higher collector temperatures which also vary in a similar manner to the solar radiation. The middle central region of the collector is heated more effectively compared to the far-left central region which shows lower temperatures suggesting more heat losses at the left edge of the collector. The collector temperatures for the case of two sunny days are shown in Fig. 4 (B1), and these show a similar variation to those of day 2 of test 1. However, there is a drop in the temperatures at 5.5 h for day 1 of test 2 due the short cloudy period around 5 h. An unexpected rise in the inlet collector temperature at around 11.2 h during day 2 for test 2 causes the other collector temperatures to also rise. This rise is likely attributed to a drop in the airflow velocity in the collector which causes the inlet temperature to rise as the airflow velocity was manually controlled at the set power supply current. These drops and rises in the airflow velocity do happen during the drying period in the collector. Very few authors have reported on this since most of the researchers assume that the airflow is constant and uniform by measuring it at the outlet of the blower which is incorrect since the airflow maybe be non-uniform. The average ambient temperatures for test 1 are 25.6 °C and 27.0 °C, respectively for the two 8 h test periods. These

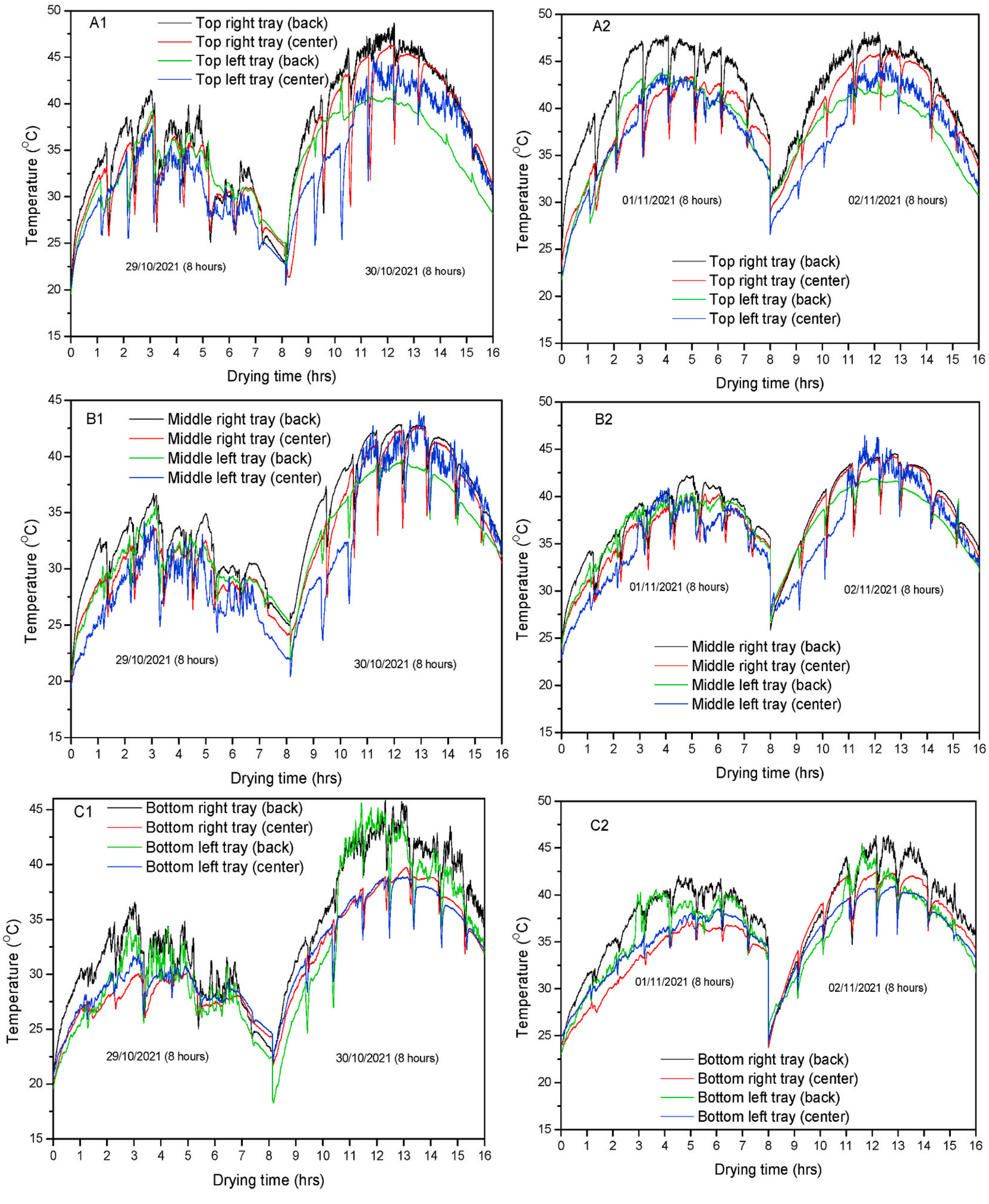

Fig. 5. Temperature profiles in the (A) top trays, (B) middle trays and the (C) bottom trays for 16 h in two consecutive days of drying with sun.

average ambient temperatures are slightly less than those for test 2 which are 30.5 °C and 28.4 °C, respectively.

Experimental temperature profiles inside the drying chamber for the two 16 h tests are shown in Fig. 5. The temperature profiles show hourly drops due to the opening of the doors in the drying chamber as the mass of the samples were measured every hour to determine the moisture ratio. For test 1, the cloudy day shows lower drying temperatures with maximum temperatures achieved at the top, middle and bottom trays being around 42, 37 and 36 °C, respectively. The top right-hand backside section (black line - Fig. 5(A1)) of the dryer shows higher temperatures implying that it is heated more effectively compared to the other sections in the top trays. The right-hand backsides of the middle and bottom trays are also more effectively heated compared to the other sections as shown by the higher temperatures. This is probably due to exiting hot air from the collector which is closer to the right-hand back side. The temperature profiles in the trays follow a similar trajectory to the variation of the global solar radiation.

For day 2 of test 1, the drying chamber temperatures are greater than those of day 1 due to the higher solar radiation conditions. The maximum temperatures in the top, middle and bottom trays are 48, 43 and 45 °C, respectively. The bottom left and right back sections achieve higher temperatures than the middle trays possibly due to non-uniform heating of the drying trays which results in the back bottom sections been heated up more effectively than the middle sections. It is also possible that heat losses in the middle section could be higher than those in the back bottom sections, but this must be confirmed with further experiments to evaluate heat losses which are beyond the scope of this study. As in the case of day 1 for test 1, the top right back section receives more heat than the other top sections for day 2 as indicated by the higher temperatures. The top left backside section shows the lowest temperature. Unlike the case of day 1, for the middle trays, the back left middle section only shows higher temperatures initially when compared to the other middle section temperatures. The temperatures in the middle section are comparable except for the back left-side middle section (Fig. 5 (B1)-green line) which shows lower temperatures. The centre sections of the bottom trays (Fig. 5(C1)- blue and red lines) show lower temperatures compared to the back sections suggesting non-uniform heating resulting in the backside section being heated more effectively compared to the centre sections.

The temperature profiles for test 2, with two consecutive days of clear conditions show the same variations as test 1. However, the drying chamber temperatures of day 1 are greater than for test 1 due to the higher amount of solar radiation since it was not cloudy on day 1 for test 2. For day 2, the drying chamber temperatures are slightly higher but comparable to those of test 1. The maximum temperatures achieved in the drying chamber for day 1 in test 2 for the top, middle and bottom trays are 48, 43 and 43 °C respectively. For day 2 in test 2, with comparable solar radiation conditions compared to day 1 and with lower wind speeds, the maximum

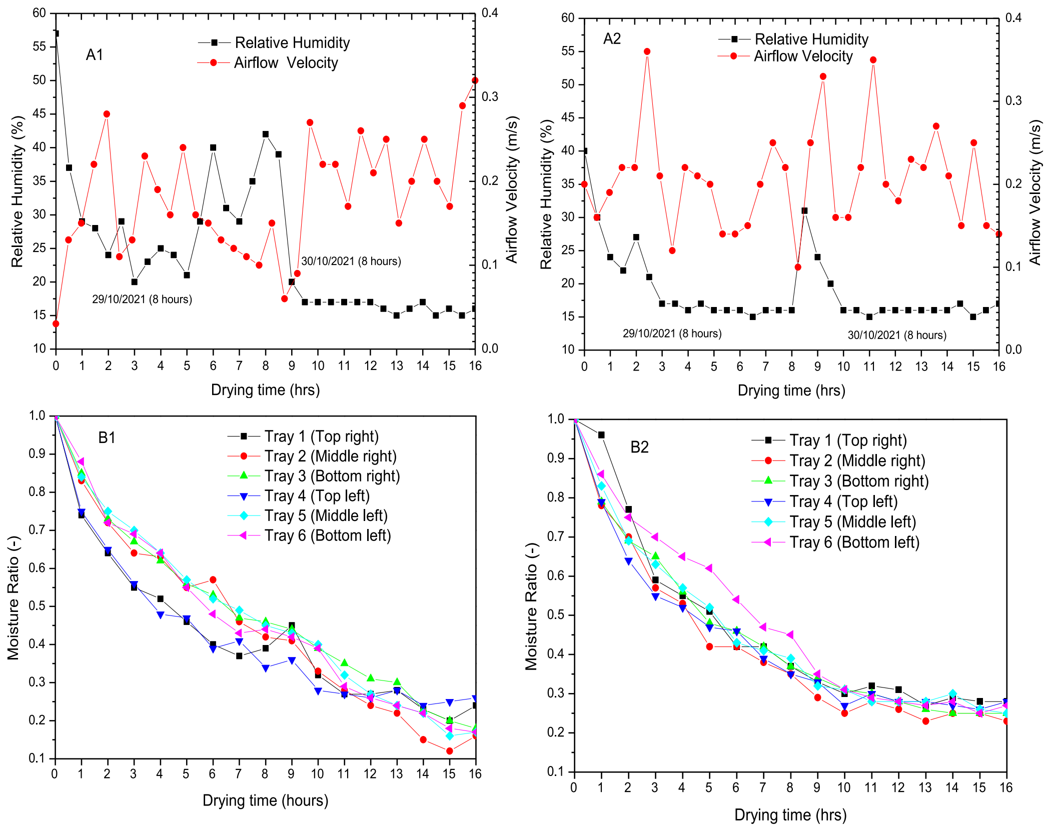

Fig. 6. (A) Relative humidity and airflow velocity profiles and (B) moisture ratio profiles in the six trays for 16 h in two consecutive days of drying with sun.

temperatures were 48, 46 and 46 °C for the top, middle and bottom trays, respectively.

The variations of the relative humidity, air flow velocity and the moisture ratio in the drying chamber are shown in Fig. 6. The airflow velocity for both tests in the chamber fluctuates up and down as the drying process progresses possibly due to the variation of the density, specific heat capacity and viscosity of the heated air in the collector. Also, pressure drops in the collector and the drying chamber could be responsible for this variation. To our knowledge, very few or no authors have measured the air flow velocity inside the drying chamber of a solar dryer. The minimum and maximum air flow velocities in the chamber for test 1 are 0.02 and 0.32 m/s, respectively. For test 2, the corresponding minimum and maximum air flow velocities are 0.09 and 0.38 m/s, respectively. The average air flow velocities for test 1 and test 2 of 0.19 and 0.21 m/s are comparable. The relative humidity for test 1 falls to a minimum of 0.20 in the first 3 h of day 1, after which it fluctuates up and down to around 0.42 at the end of day 1 due to the overcast conditions during the day. In contrast to this, for day 1 in test 2 which is generally sunny, the relative humidity falls from 0.40 to around 0.16 at the end of 8 h. For day 2 in both tests, the relative humidity decreases with the increase in the drying time. The relative humidity decreases from 0.40 to around 0.15 at the end of day 2 for test 1 which is very similar to the decrease from 0.32 to around 0.16 for test 2. Clear solar radiation conditions reduce the relative humidity in the drying trays due the higher temperatures attained. There is also humidity build up during the night due to the lower night-time temperatures which explains why the relative humidity starts at higher values at the beginning of the tests on day 2.

The moisture ratio profiles for tests 1 and 2 are shown in Fig. 6 (B). For test 1, its clear that the top trays (blue and black lines) dry up faster than the other trays during the first day achieving moisture ratios close to 0.40 on the end of day 1. The other trays achieve moisture ratios of around 0.48 at the end of day 1 for test 1. There is moisture build up at the top right tray overnight which results in a higher moisture ratio for the top right tray at the start of drying for test 1 on day 2. At the end of day 2, the moisture ratios are around 0.27 for the top trays and 0.18 for the middle and bottom trays for test 1. This suggests that the rate of drying slows down at the top trays for day 1 of test 1 possibly due to some reabsorption of moisture due to the fluctuating air flow velocity which affects the top trays more than the bottom trays. For test 2, the top left tray (blue line) shows the fastest drop in moisture ratio for day 1 suggesting that it is more effectively heated than the other trays. In contrast to test 1, the top right tray (black line) shows the slowest drop during the first 2 h suggesting non-uniform heating at the top during this period. However, for day 1 (test 2), the moisture ratios uniformize at the end of the 8 h drying period with moistures ratios dropping to 0.35 except for the bottom left which shows a higher moisture ratio of 0.45. For day 2, during test 2, the moisture ratios are relatively comparable suggesting more uniform drying with moisture ratios ranging from 0.25 to 0.30 at the end of day 2. This is contrast to day 2 for test 1 which was a cloudy day followed by a sunny day where there are larger moisture ratio differences. The variable moisture ratios in different trays have rarely been investigated and these results provide a useful insight into the drying kinetics in the different sections of solar food dryers.

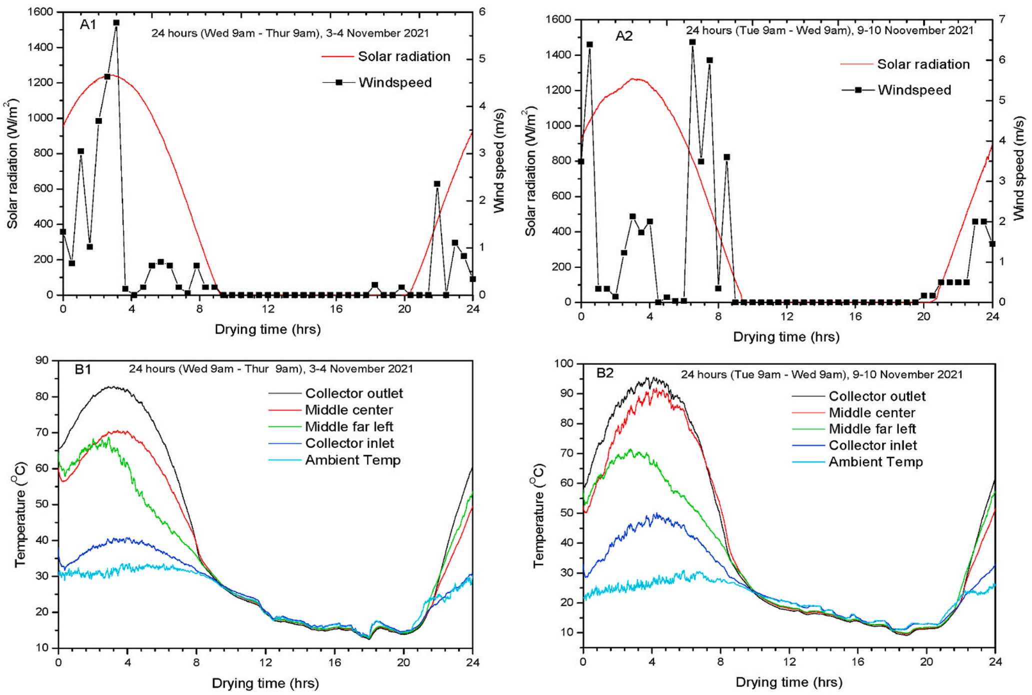

Fig. 7. (A) Global solar radiation and wind speed profiles and, (B) collector and ambient temperatures for continuous 24 h drying with and without the sun.

4.2. 24 h solar drying tests

Solar radiation, wind speed and thermal profiles in the collector during continuous 24 h drying cycles are shown in Fig. 7 (A, B) during sunny days with high (0.23 m/s- Fig. 7A) and low (0.11 m/s-Fig. 7B) average drying chamber air flow velocities. In both tests, the maximum solar radiation is around 1250 W/m^2, which occurs around 3 h from the commencement of the drying process. The solar radiation starts to rise after 20 h on day 2 achieving maximum values close to 800 W/m^2 at the end of the 24 h cycles for both cases. The wind speeds are also comparable with maximum wind speeds of around 5.8 and 6.5 m/s for the high and low average drying chamber air flow velocities. For the high air flow velocity, the maximum collector outlet temperature is around 84 °C, compared to around 95 °C for the low airflow velocity due to less resident time in the collector for the high air flow velocity. The middle centre collector temperature achieves a higher maximum temperature of around 90 °C for the low airflow velocity compared to 70 °C for the high airflow velocity. Generally, higher collector temperatures are seen with the lower airflow velocity compared to the higher airflow velocity.

The temperature profiles in the six trays for the continuous 24 h drying cycles are shown in Fig. 8 (A-C). Slightly higher top tray temperatures (Fig. 8 (A1, A2)) are achieved with the lower average airflow velocity due the higher collector temperatures attained. The minimum temperature attained overnight for the higher average airflow velocity at the top trays is around 7.5 °C, which is around 2.5 °C greater than that of the lower average airflow velocity. This suggests that the higher average airflow velocity is slightly more

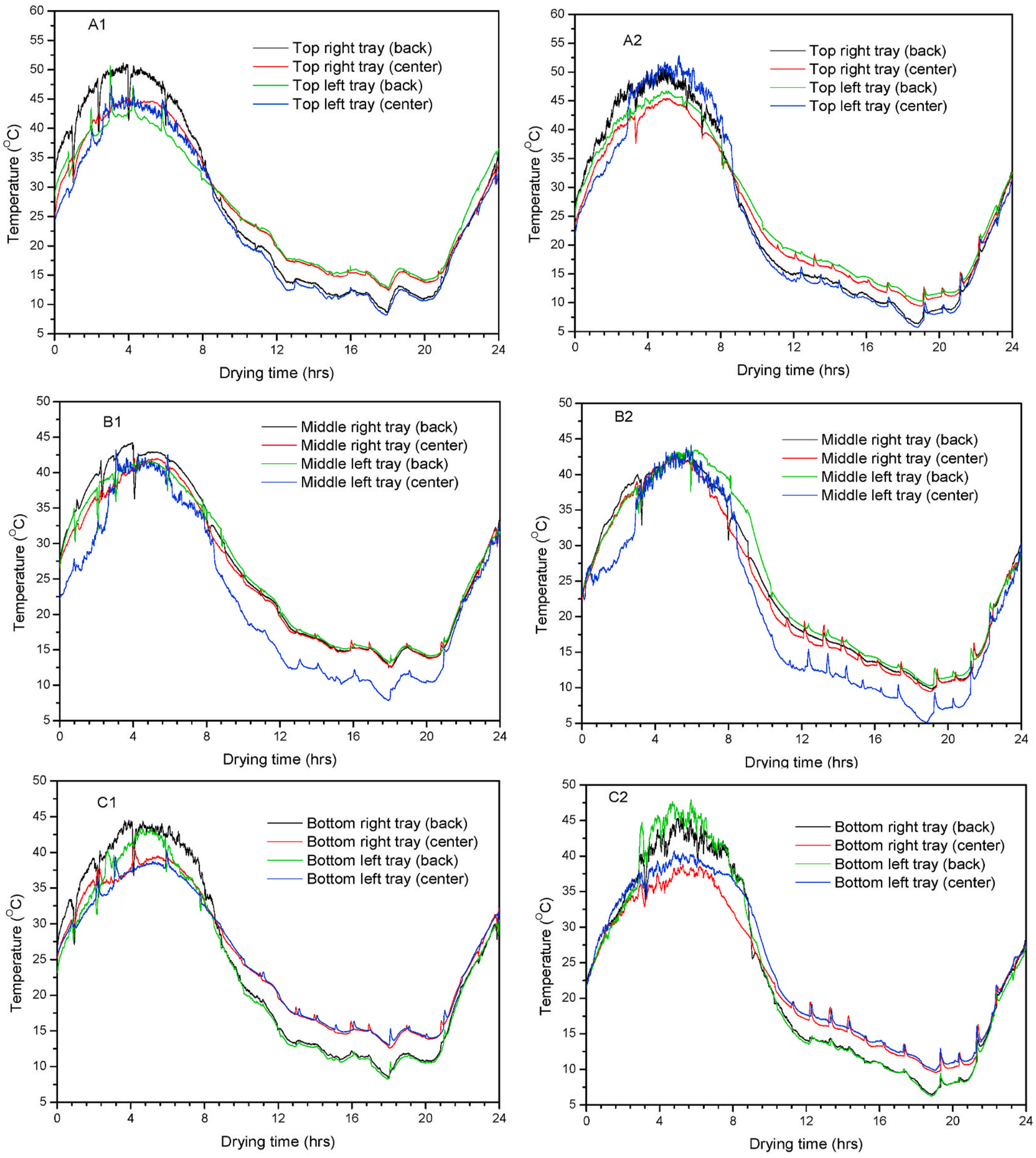

Fig. 8. Temperature profiles in the (A) top trays, (B) middle trays and the (C) bottom trays for continuous 24 h drying with and without the sun.

effective in drying overnight compared to the lower average airflow velocity. The minimum temperatures in all levels of the dryer are also generally higher for the higher average airflow velocity further showing that better overnight performance is exhibited by the higher average airflow velocity. The middle and bottom level drying chamber temperatures (Fig. 8 (B–C)) are comparable for both cases during the solar drying period. Maximum temperatures attained in the drying chamber after overnight drying are slightly higher for the higher average airflow velocity suggesting better performance compared to the lower average airflow velocity. In comparison to the 8 h tests, the drying temperatures are slightly higher for the 24 h tests due to the slightly higher solar radiation conditions and possibly because of the lower wind speeds which reduced the induced heat losses.

Airflow velocities, relative humidities and moisture ratios in the drying chamber for the 24 h tests are shown in Fig. 9 (A, B). The airflow velocities fluctuate up and down in a similar manner to the 8 h tests on two consecutive days. For the higher average airflow velocity, the minimum and maximum airflow velocities are about 0.04 and 0.35 m/s, respectively. For the lower average airflow velocity, the minimum and maximum airflow velocities are around 0.01 and 0.24 m/s, respectively.

The relative humidity for the higher average air flow velocity drops from 38 % at the start of the drying process to around 16 % during the first 8 h of sunshine. Due to moisture rebuilding at night, the relative humidity rises to a maximum of around 55 % at 21 h of drying, gradually falling during the next sunny day to 30 % at 23 h. For the higher average airflow velocity, the initial relative humidity is higher (43 %). It drops fluctuating up and down to a minimum of around 20 % in 10 h, and then rises to a maximum of about 44 % overnight after 18 h of drying. The relative humidity then drops to around 24 % for the next sunny day at 24 h of the drying process. There is no real solid corelation between the airflow velocity and the relative humidity, however, higher fluctuating airflow velocities tend to increase the relative humidity for both cases. Also, generally higher relative humidities are seen with the lower average airflow velocity compared to the lower average airflow velocity. The relative humidities for the 8 h tests are obviously lower than those of the 24 h tests due to the higher solar radiation conditions in the 8 h tests.

The moisture ratio plots shown in Fig. 9 (B) show that the top trays dry up faster in both cases, and the drying process continues overnight regardless of the higher relative humidity and lower drying chamber temperatures. After 8 h of drying, the moisture ratios for the top trays are around 0.39 (Top left) and 0.35 (Top right) for the higher average airflow velocity compared to 0.45 (Top left) and 0.38 (Top left) for the lower average airflow velocity. This suggests the that the higher average air velocity enhances the drying process during sunshine hours. The middle and bottom trays also show lower moisture ratios after 8 h of drying for the higher average airflow velocity case compared to the lower average airflow velocity case. The final moisture ratios at the end of 24 h range between 0.29 and

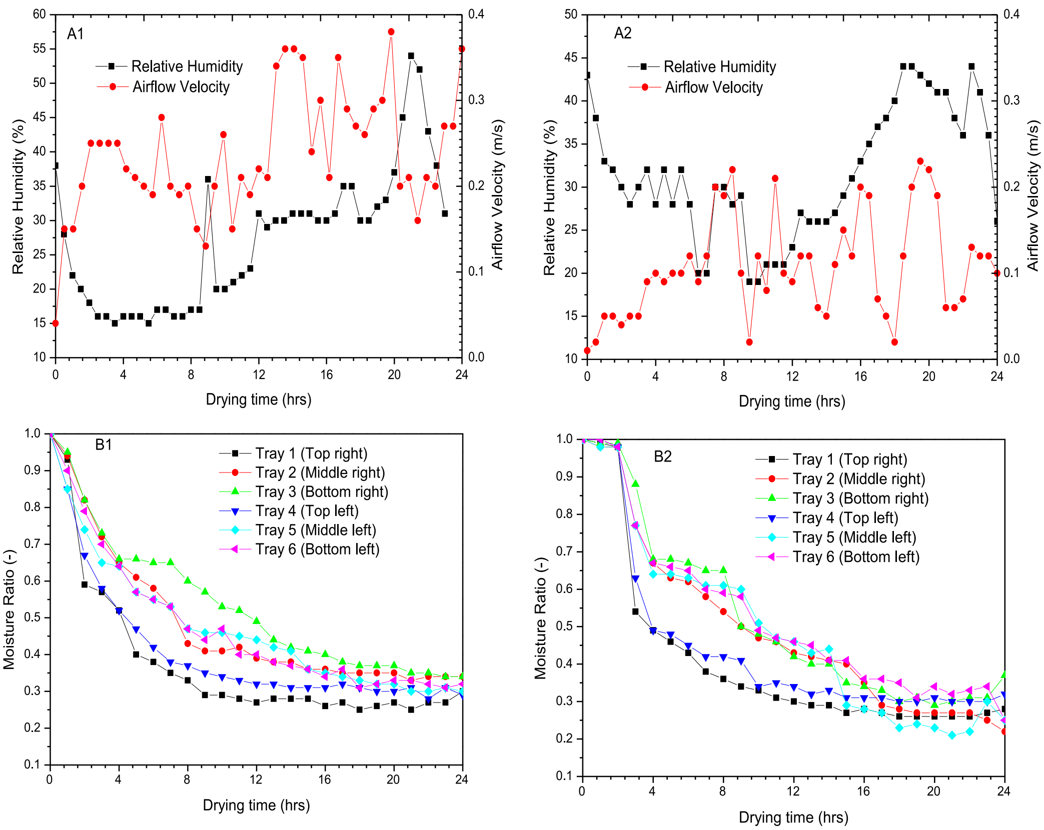

Fig. 9. (A) Relative humidity and airflow velocity profiles and (B) moisture ratio profiles in the six trays for continuous 24 h drying with and without the sun.

0.35 for the higher average airflow velocity. This is comparable to the low airflow velocity case which ranges between 0.25 and 0.39.

4.3. Comparison of average thermal performance parameters

Fig. 10 shows a comparison of average thermal performance parameters for the four different tests calculated using the moving average values of the solar radiation and the air flow velocity. Test 3 and test 4 (Fig. 10 (A)) show comparable and higher average solar input powers ranging between a minimum of 2000 W and maximum of around 2350 W. Test 1 (day 1) which is a cloudy day, shows a general decrease in the solar input power from 2400 to 1200 W at the end of 8 h. Test 2 shows slightly lower average solar power values for day 1 compared to tests 3 and 4. During day 2, the average solar input powers for tests 1 and 2 comparable. The moving average airflow velocities shown in Fig. 10 (B) show different variations indicating different flow regimes in the collector which has been rarely reported in previous studies. Test 2 shows higher average air flow velocities which decrease steadily from around 1.2 m/s to 0.8 m/s at the end of 16 h. On the other hand, test 1 shows an increase to a steady state value of around 0.65 m/s between 4 and 8 h on day 1. For day 2, test 1 show an initial rapid increase and fall between 8 and 10 h. This is followed by a slow steady increase from 10 to 15 h. For the 24 h tests, during the solar drying period, the average airflow velocity rises from around 0.15 m/s to become 0.65 m/s at the end of 8 h which is comparable to test 2 at the day 1. Test 4 shows the lowest average airflow velocity which rises slowly from around 0.10 m/s to around 0.20 m/s at the end of 8 h.

Average collector power outputs are shown in Fig. 10(C). All the output powers show a similar trend of rising and falling for all test cases. As a result of the higher moving average airflow velocity for test 2, it shows higher output power profiles which peak and fall for days 1 and 2. The maximum average output powers for test 2 are around 1800 and 1650 W, respectively, for days 1 and 2. As a result of the cloudy conditions of day 1 of test 1, the average output power fluctuates, and it shows a maximum value of around 1100 W. The average output power profile for day 2 for test 1 is comparable to that of test 2, however its maximum value of around 1400 W is lower than test 2 (1650 W). Test 4 with the lowest moving average airflow velocity shows the lowest output power achieving a maximum power of only 250 W after 6 h. The average collector thermal efficiencies (Fig. 10 (D)) show the same trends as the average output collector powers. Test 2 show higher average collector thermal efficiencies due to its higher moving average airflow velocities, while test 4 with the lowest moving average airflow velocities show the lowest average collector thermal efficiencies. The maximum average collector efficiencies for tests 1, 2, 3 and 4 are around 0.6, 0.8, 0.4 and 0.1, respectively. The collector efficiency is highly influenced by the moving average airflow velocity, and it increases with an increase in the moving average airflow velocity.

The average solar drying efficiencies are shown in Fig. 11. All drying efficiencies initially peak to maximum values then gradually fall fluctuating up and down except of the case 4 which falls without up and down fluctuations. These fluctuations are an indication of non-unform drying as result of different airflow velocity regimes in the drying chamber. Test 4 with the lowest moving average airflow

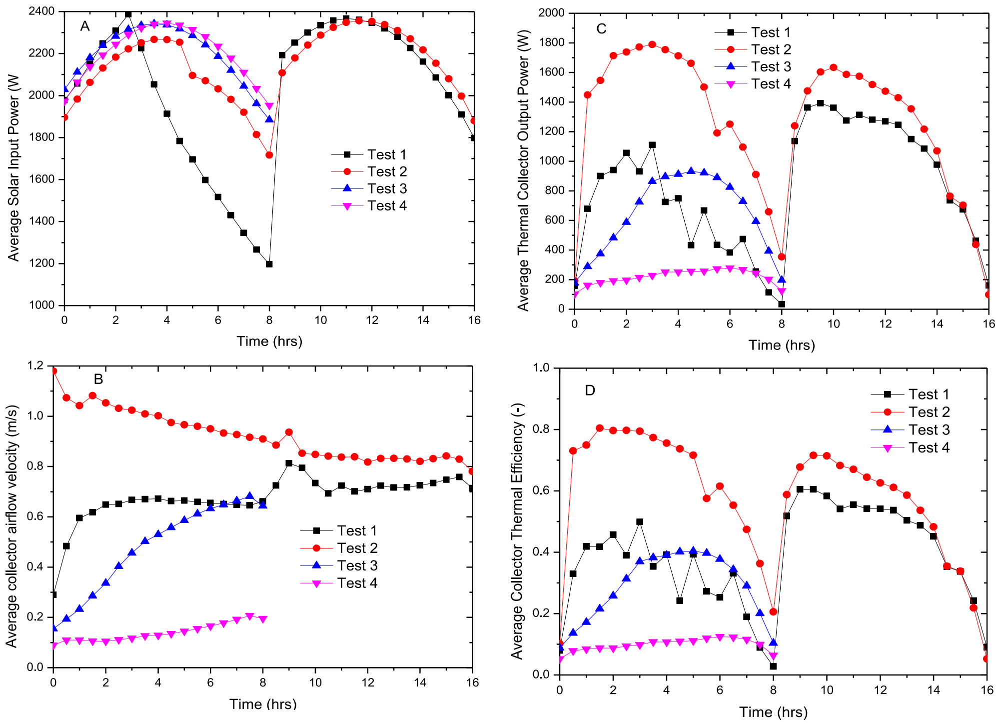

Fig. 10. (A) Average solar input power, (B) collector airflow velocity, (C) thermal collector output power and (D) collector thermal efficiency for the four different cases.

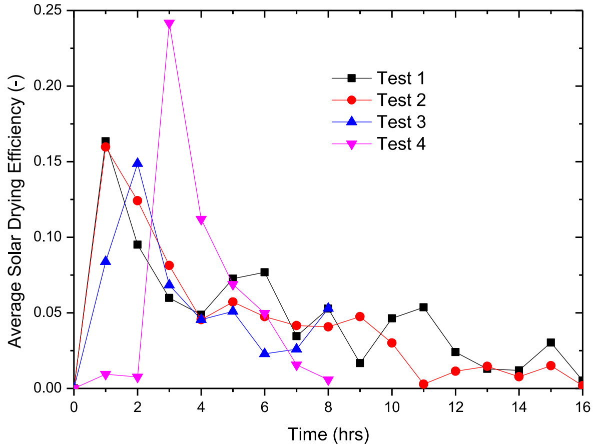

Fig. 11. Average solar drying efficiencies for the four test cases.

shows the highest drying efficiency at 3 h regardless of its lower collector moving average airflow velocity because of the rapid drop in the moisture content of the top trays (Fig. 9(B2)) possibly induced by a larger non-uniform airflow regime at the top trays during the same period compared to the other cases. This suggests that the airflow velocities should measured at different locations in the drying trays to fully understand the drying kinetics. The assumption that the airflow rate is constant inside the dryer and in the collector is not very valid, and it should be taken cautiously especially when low airflow velocities are considered. Tests 1 and 2 show similar maximum solar drying efficiencies of around 0.16 during the first hour of drying whereas the maximum solar drying efficiency of 0.15 obtained after 2 h of drying for test 3 which is comparable to that of test 1 and 2. For tests 1, 2, 3 and 4 on day 1, the average drying efficiencies for the total solar drying period are 6.9, 6.9, 5.5 and 5.7 % respectively. Comparable values of the average drying efficiencies suggest that the average collector powers, airflow velocities and efficiencies have a very insignificant effect on the average solar drying efficiency for the whole drying period. For day 2 in tests 1 and 2, the average drying solar drying efficiencies for the total solar drying period are 2.8 and 1.9 % indicating a reduction in the moisture removal rate during day 2.

To compare properly the performance of the four cases, average moisture ratios in the drying chamber are plotted in Fig. 12. The consecutive 8 h tests on two days show lower moisture ratios at the end of 16 h with test 1 (cloudy and sunny day) showing a final moisture ratio of 0.20 and test 2 (two sunny days) showing a final moisture ratio of 0.26. Test 2 shows a fast rate of drop in the moisture ratio in the first 12 h of drying due to the higher average airflow velocity. Higher average moisture ratios are seen with the 24 h tests. Test 3 with a higher airflow velocity shows a faster rate of drop in the moisture ratio from 0 to 14 h due to the high rate of moisture removal when comparing the 24 h tests. However, for test 4 between 2 and 4 h, the moisture ratio drops drastically which causes a very large increment in the solar drying efficiency depicted in Fig. 11 during the same period. At the end of 24 h, the average moisture ratio for the lower average airflow velocity is slightly lower (0.28) compared to 0.32 for the higher average airflow velocity.

4.4. Comparison of previous work and the quality of the dried product

Table 1 shows a comparison of the current work for solar of drying bananas with previous recent work done by other researchers.

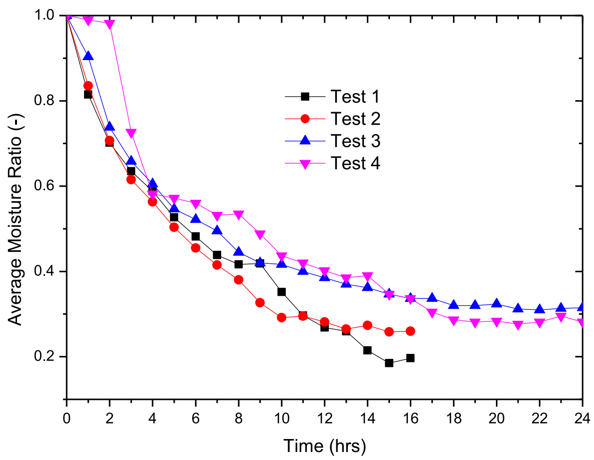

Fig. 12. A comparison of the average moisture ratios for the four test cases.

Table 1
A comparison of recent work done on the performance of solar drying of bananas.

Author and Year	Drying Time (Hrs)	Mass of Banana Slices (kg)	Average final moisture ratio/content (–)
Mawire et al. (2023)-Present Work (Cloudy and Sunny Days, 16 h test)	16	3.18	0.202
Mawire et al. (2023)-Present Work (Two Sunny Days, 16 h test)	16	3.18	0.237
Mawire et al. (2023)-Present Work (Low average airflow velocity-0.11 m/s)	24	3.18	0.282
Mawire et al. (2023)-Present Work (Low average airflow velocity-0.23 m/s)	24	3.18	0.323
El-Sebaey et al. (2023) [32]	11	1.00	0.106
Mutabilwa and Nwaigwe (2020) [24]	9	Not mentioned	0.200
Nabnean and Nimnuan (2020) [21]	40	10.00	0.280
Pruengam et al. (2021) [23]	32	10.00	0.200
Arun et al. (2019) [25]	10	20.00	0.160
Hegde et al. (2015) [22]	16	Not mentioned	0.28–0.37 (0.5, 1.5 and 2 m/s)

The experimental load varied from 0.24 to 20 kg, and the drying time ranged between 9 and 40 h. The average moisture presented in this work is comparable to the work other researchers. However, the overnight performance presented in our study can be improved with the use thermal energy storage (TES).

Fig. 13 shows banana slices after a solar drying experiment. The colour, taste, texture, and quality of the dried bananas was reasonably good.

Fig. 14(a–c) shows a comparison of fresh banana slices with those of the 16 h and 24 h tests. The dried banana slices for the two tests are almost identical, and they show a crispy yellow colour (little darkening) with very little deformation from the original shape implying that a quality product has been produced. Additionally, overnight changes in the relative humidity due to low drying temperatures seem not to affect the quality as no noticeable blackening is observed in the samples after 24 h of drying. Continuous 24-h and batch drying in two 8 h periods seems to produce the same quality of products which justifies using the solar dryer for 24 h unlike previous work [20–29] which only considers solar drying of bananas during sunshine periods. Pre-treatment with lemon juice seems to be an effective method of preventing bacterial growth for the two cases of drying. It is also important to state that the dried banana slices were placed in vacuum-sealed plastics after each drying process and refrigerated to further extend their shelf-life.

A photographic comparison of our dried banana slices and the limited reported experimental solar drying cases of bananas is shown in Fig. 15(a–c). Our banana slices (Fig. 15(a)) have the same shape as those reported in the literature. In terms of colour, banana slices reported by Wakjira et al. [26] (Fig. 15 (b)) are darker than ours although the authors reported that this was their best quality. Wakjira et al. [26] reported that the blackening of bananas is an indication of microbacterial growth. Our banana slices are yellower compared to those reported by Hedge et al. [22] (Fig. 15 (c)) who reported a similar quality to those of Wakjira et al., [26]. Our banana slices have a yellower and more appealing colour possibly due to pretreatment with lemon juice before the drying experiment.

As mentioned already in the introduction, no reported work on solar drying of bananas has compared experimental products with commercially available products. A photographic comparison of our dried product (Fig. 16(d)) and commercially available products in South Africa is shown in Fig. 16. Our product is lighter and more appealing than the Tierhoek organic dried bananas (Fig. 16(c)) [38] which were possibly untreated and dried in the open sun. The Naturalz Kerala banana chips made in coconut oil (Fig. 16(a)) [36] are yellower and crispier than our product possibly due to treatment with coconut oil. Gaby's banana chips (Fig. 16(b)) are much lighter than our product which is an indication of no prior treatment, but the taste was the same with our product. Gaby's banana chips were the only product that could be compared in taste with our product. Our dried banana slices show more or less the same shape as all

Fig. 13. A photograph of the dried banana slices in a tray.

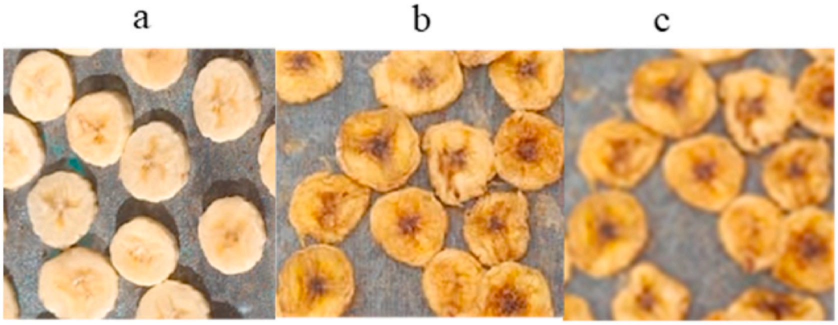

Fig. 14. A photograph of (a) fresh bananas, (b) bananas dried in a 16-hr test and (c) bananas dried in a 24-hr test.

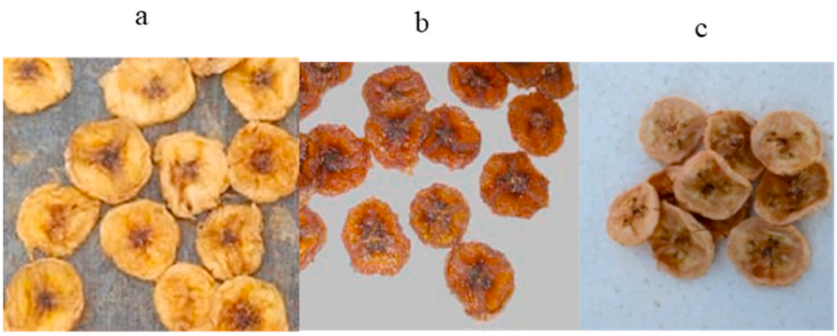

Fig. 15. A photographic comparison of (a) our dried banana slices, (b) banana slices dried by Wakjira et al. [26] and (c) banana slices dried by Hedge et al. [22].

Fig. 16. A photographic comparison of (a) commercial Naturalz Kerala banana chips made in coconut oil [36], (b) Gaby's banana chips [37], (c) Tierhoek organic dried bananas [38], and (d) our dried banana slices.

commercially available products.

It is also important to note that most commercially available products are dried in electrical dryers which is quite expensive for developing countries. In developing countries, especially in rural areas, electricity supply is limited which justifies the usage of solar dryers with free energy from the sun to prevent post-harvesting losses and associated problems of open sun drying like insect infestation, loss of nutrients and colouring and contamination due to dust. The proposed dryer can operate for 24 h continuously without storage unlike previously reported dryers for bananas [20–29] where moisture removal overnight is not possible. The 24-h operation is like an electrical dryer which operates continuously. However, an electrical dryer requires a continuous supply of electrical energy which is a luxury in the developing world. The cost of our dryer is around R 8000 (USD 420) because of its larger size. It can be scaled down to half or a third of the price for small community subsistence farmers in the developing world. The cost is still a bit cheaper than electrical commercially available food dryers (R 8995 (USD 470)) [39] which require the continuous supply of electrical energy which is a luxury in most parts of rural sub-Saharan Africa.

5. Conclusion

An experimental setup of an indirect solar dryer for drying banana slices was presented to evaluate its performance under different drying conditions. The novel issues of the dryer included measuring the airflow velocity in the drying chamber, multiple thermal profiles in the different trays and the relative humidity under different conditions. The first two tests were 8 h tests (16 h in total) on two consecutive days. Test 1 was carried out on a cloudy day followed by a sunny day with an average airflow velocity of 0.19 m/s in the drying chamber, whereas test 2 was carried on two consecutive sunny days using an almost similar average airflow velocity of 0.21 m/s. The next two tests were continuous 24 h tests with high (0.23 m/s) and low (0.11 m/s) average airflow velocities in the drying chamber under good solar radiation conditions.

The main conclusions of the study were:

1. For the 16 h tests, the maximum temperatures obtained in the collector and the drying chamber were around 80 and 48 °C, respectively. The cloudy conditions lowered the collector and drying chamber temperatures. For the 24 h tests, maximum collector temperatures were around 84 and 95 °C for the high and low average airflow velocity, and the corresponding maximum drying chambers were around 50 °C for both tests. The higher temperatures for 24 h tests can be attributed to the higher solar radiation conditions and possibly to lower wind speed variability in the 24 h tests thus reducing heat losses.
2. The airflow velocities in all 4 tests fluctuated up and down in the drying chamber possibly due to the variation of the density, specific heat capacity and viscosity of the heated air in the collector. Also, pressure drops in the collector and the drying chamber could be responsible for this variation.
3. The relative humidities for both 16 h tests at the end of day 2 (15 and 16 %) are lower than those of the 24 h tests (30 and 26 %) due to moisture rebuilding overnight because of lower night temperatures. Even with these lower night temperatures for the 24 h tests, the drying process continued with moisture removal from the bananas.
4. The final average moisture ratios for the 16 h tests were 0.20 (cloudy and sunny days) and 0.26 (two sunny days). These final moisture ratios were lower than those obtained for the 24 h tests which were 0.32 (high airflow velocity) and 0.28 (low airflow velocity), respectively. An increase in the drying chamber airflow velocity for the 24 h tests, resulted in faster moisture removal during sunshine hours.
5. The maximum average collector efficiencies for tests 1, 2, 3 and 4 were around 0.6, 0.8, 0.4 and 0.1, respectively. The collector efficiency was highly influenced by the moving average airflow velocity, and it increased with an increase in the moving average airflow velocity.
6. For tests 1,2,3 and 4 on day 1, average drying efficiencies for the total solar drying period were 6.9, 6.9, 5.5 and 5.7 %, respectively. These drying efficiencies were comparable suggesting that the average collector powers, airflow velocities and efficiencies had a very insignificant effect on the average solar drying efficiency for the whole drying period. For day 2 for test 1 and 2, the average drying solar drying efficiencies for the total solar drying period were 2.8 and 1.9 % indicating a reduction in the moisture removal rate during day 2.
7. The quality of our dried product in terms of colour and shape was comparable both to previously reported and commercially available products.

For future work, the collector could be embedded with latent heat storage to improve the drying performance at night. The collector could also be incorporated with fins to improve heat transfer and increase the outlet temperature obtained thus speeding up the drying process. Different products need to be simultaneously dried in the dryer to evaluate its versatility.

Data availability statement

The data presented in this paper are available only on request from the authors.

CRediT authorship contribution statement

Ashmore Mawire: Writing – review & editing, Writing – original draft, Supervision, Resources, Project administration, Methodology, Funding acquisition, Formal analysis, Conceptualization. **Masodi Ramokali:** Writing – review & editing, Writing – original draft, Validation, Methodology, Investigation, Formal analysis, Data curation, Conceptualization. **Molebogeng Mothupi:** Writing – review & editing, Writing – original draft, Methodology, Investigation, Formal analysis, Data curation, Conceptualization. **Maarten Vanierschot:** Writing – review & editing, Writing – original draft, Supervision, Project administration, Methodology, Funding acquisition, Formal analysis, Data curation, Conceptualization.

Declaration of competing interest

The authors declare the following financial interests/personal relationships which may be considered as potential competing interests:Ashmore Mawire reports financial support and travel were provided by VLIR-UOS, Belgium under the South Initiatives 2020 project (Project No: ZA2020SIN306A101), that includes: funding grants. Ashmore Mawire has no patent to report.

Acknowledgements

Mr Thys Taljaard, the head of the Instruments Making Department of North-West University and his technicians are acknowledged for fabrication of the experimental setup. Additionally, the authors acknowledge VLIR-UOS, Belgium for funding to conduct the research under the South Initiatives 2020 project (Project No: ZA2020SIN306A101).

References

[1] T.K. Rudel, P. Meyfroidt, Organizing anarchy: the food security–biodiversity–climate crisis and the genesis of rural land use planning in the developing world, Land Use Pol. 36 (2014) 239–247.
[2] M.D. Rahman, I. Khan, D.L. Field, K. Techato, K. Alamen, Powering agriculture: present status, future potential, and challenges of renewable energy applications, Renew. Energy 188 (2022) 731–749.
[3] A. Awad, The determinants of food insecurity among developing countries: are there any differences? Scientific African 19 (2023) e01512.
[4] J. Gustavsson, C. Cederberg, U. Sonesson, FAO Global Food Losses and Waste. Extent Causes and Prevention, 2011, pp. 1–37. Rome.
[5] M.H. Ahmed, D. Vasas, A. Hassan, J. Molnár, The impact of functional food in prevention of malnutrition, PharmaNutrition 19 (2022) 100288.
[6] A. Kamarulzaman, M. Hasanuzzaman, N.A. Rahim, Global advancement of solar drying technologies and its prospects: a review, Sol. Energy 221 (2021) 559–582.
[7] V.R. Mugi, P. Das, R. Balijepalli, V.P. Chandramohan, A review of natural energy storage materials used in solar dryers for food drying applications, J. Energy Storage 49 (2022) 104198.
[8] P. Udomkun, S. Romuli, S. Schock, B. Mahayothee, M. Sartas, T. Wossen, E. Njukwe, B. Vanlauwe, J. Müller, Review of solar dryers for agricultural products in Asia and Africa: an innovation landscape approach, J. Environ. Manag. 268 (2020) 110730.
[9] A.B. Lingayat, V.P. Chandramohan, V.R.K. Raju, V. Meda, A review on indirect type solar dryers for agricultural crops – dryer setup, its performance, energy storage and important highlights, Appl. Energy 258 (2020) 114005.
[10] G. Srinivasan, D.K. Rabha, P. Muthukumar, A review on solar dryers integrated with thermal energy storage units for drying agricultural and food products, Sol. Energy 229 (2021) 22–38.
[11] E. Getahun, M.A. Delele, N. Gabbiye, S.W. Fanta, P. Demissie, M. Vanierschot, Importance of integrated CFD and product quality modeling of solar dryers for fruits and vegetables: a review, Sol. Energy 220 (2021) 88–110.
[12] R. Embong, N. Shafiq, KusbiantoroA, M.F. Nuruddin, Effectiveness of low-concentration acid and solar drying as pre-treatment features for producing pozzolanic sugarcane bagasse ash, J. Clean. Prod. 112 (2016) 953–962.
[13] W.B. Chaouch, A. Khellaf, A. Mediani, M.E. Slimani, A. Loumani, A. Hamid, Experimental investigation of an active direct and indirect solar dryer with sensible heat storage for camel meat drying in Saharan environment, Sol. Energy 174 (2018) 328–341.
[14] H. Essalhi, M. Benchrifa, R. Tadili, M.N. Bargach, Experimental and theoretical analysis of drying grapes under an indirect solar dryer and in open sun, Innovative Food Sci. Emerging Technol. 49 (2018) 58–64.
[15] F. Ullah, M. Kang, Impact of air flow rate on drying of apples and performance assessment of parabolic trough solar collector, Appl. Therm. Eng. 127 (2017) 275–280.
[16] S. Janjai, N. Lamlert, P. Intawee, B. Mahayothee, B.K. Bala, N. Nagle, J. Muller, Experimental and simulated performance of a PV-ventilated solar greenhouse dryer for drying of peeled longan and banana, Sol. Energy 83 (2009) 1550–1565.
[17] K.B. Koua, W.F. Fassinou, P. Gbaha, S. Toure, Mathematical modelling of the thin layer solar drying of banana, mango, and cassava, Energy 34 (2009) 1594–1602.
[18] B.K. Bala, M.R.A. Mondol, B.K. Biswas, B.L. Das Chowdury, S. Janjaic, Solar drying of pineapple using tunnel drier, Renew. Energy 28 (2003) 183–190.
[19] A. Viljoen, K. Kunert, A. Kiggundu, J.V. Escalant, C.H. Bornman, Biotechnology for sustainable banana and plantain production in Africa: the South African contribution, South Afr. J. Bot. 70 (2004) 67–74.
[20] B.M.A. Amer, M.A. Hossain, K. Gottschalk, Design and performance evaluation of a new hybrid solar dryer for banana, Energy Convers. Manag. 51 (2010) 813–820.
[21] S. Nabnean, P. Nimnuan, Experimental performance of direct forced convection household solar dryer for drying banana, Case Stud. Therm. Eng. 22 (2020) 100787.
[22] V.M. Hegde, V.S. Hosur, S.K. Rathod, P.A. Harsoor, K.B. Narayana, Design, fabrication, and performance evaluation of solar dryer for banana, Energy, Sustainability and Society 5 (2015) 23.
[23] P. Pruengam, S. Pathaveerat, P. Pukdeewong, Fabrication and Testing of double-sided solar collector dryer for drying banana, Case Stud. Therm. Eng. 27 (2021) 101335.
[24] P.X. Mutabilwa, K.N. Nwaigwe, Experimental evaluation of drying of banana using a double-pass solar collector (DPSC) and theoretical analysis using a CFD model, Cogent Engineering 7 (2020) 1789363.
[25] K.R. Arun, M. Srinivas, C.A. Saleel, S. Jayaraj, Active drying of unripened bananas (Musa Nendra) in a multi-tray mixed mode solar cabinet dryer with backup energy storage, Sol. Energy 188 (2019) 1002–1012.
[26] M. Wakjira, D. Adugna, G. Berecha, Determining slice thickness of banana (Musa spp.) for enclosed solar drying using solar cabinet dryer under Ethiopian condition, Am. J. Food Technol. 6 (2011) 568–580.
[27] F. Narsi, Solar thermal drying performance analysis of banana and peach in the region of Gafsa (Tunisia), Case Stud. Therm. Eng. 22 (2022) 100771.
[28] A. Lingayat, V.P. Chandramohan, V.R.K. Raju, Design, development, and performance of indirect type solar dryer for banana drying, Energy Proc. 109 (2017) 409–416.
[29] A. Lingayat, V.P. Chandramohan, Numerical investigation on solar air collector and its practical application in the indirect solar dryer for banana chips drying with energy and exergy analysis, Therm. Sci. Eng. Prog. 26 (2021) 101077.
[30] P.D. Tegenaw, A. Mawire, M. Ramokali, M. Mothupi, M. Vanierschot, Experimental measurement of heat transfer in a solar powered food dryer, in: Southern African Sustainable Energy Conference (SASEC2021), Spier, Stellenbosch, South Africa, 2021.
[31] A. Djebli, S. Hanini, O. Badaoui, B. Haddad, A. Benhamou, Modeling and comparative analysis of solar drying behavior of potatoes, Renew. Energy 145 (2020) 494–1506.
[32] M.S. El-Sebaey, S.M.T. Mousavi, S. El-Din, F.A. Essa, An experimental case 39study on development the design and the performance of indirect solar dryer type for drying bananas, Sol. Energy 255 (2023) 50–59.
[33] A. Kushwah, A. Kumar, M.K. Gaur, Optimization of drying parameters for hybrid indirect solar dryer for banana slices using response surface methodology, Process Saf. Environ. Protect. 170 (2022) 176–187.
[34] R.V. Mugi, M.C. Gilago, V.P. Chandramohan, Performance studies on indirect forced convection solar dryer without and with thermal energy storage during drying muskmelon slices, J. Therm. Anal. Calorim. 148 (2023) 9201–9216.
[35] M. Mawire, K. Lentswe, P. Owusu, A. Shobo, J. Darkwa, J. Calautit, M. Worall, Performance comparison of two solar cooking storage pots combined with wonderbag slow cookers for off-sunshine cooking, Sol. Energy 208 (2021) 1166–1180.
[36] Naturalz Kerala banana chips. https://www.desertcart.co.za/products/227316844-naturalz-kerala-banana-chips-made-in-coconut-oil-250g website accessed in October 2023.

[37] Gaby's banana chips. https://www.dischem.co.za/gaby-s-banana-chip-250g-026 website accessed in October 2023.
[38] Tierhoek organic dried bananas. https://www.organicchoice.co.za/product/organic-dried-bananas-tierhoek-organic-farm website accessed in October 2023.
[39] Excalibur Dehydrator. https://www.naturalwise.co.za/-Excalibur-Dehydrator-9-Tray-with-26-hour-built-in-timer website accessed in October 2023.